# Communicating Radar using FSK and Fractional Fourier Transform for Automotive Applications

Pasquale Striano, Christos V. Ilioudis, Carmine Clemente and John J. Soraghan
Centre for Signal and Image Procesing, University of Strathclyde, Glasgow, United Kingdom
E-mail: pasquale.striano, c.ilioudis, carmine.clemente, j.soraghan- @strath.ac.uk

***Abstract*—In modern radar applications, such as automotive, integration of radar and communications has become an important requirement. Systems able to provide joint radar and communications would exploit the same hardware while providing enhanced capabilities to the carrying platform, such as road situation awareness and content sharing. In this paper a novel framework for automotive radars based on the Fractional Fourier Transform (FrFT) for waveform design is introduced. The aim of the proposed approach is to preserve radar performance while integrating a communication link. Simulation results demonstrate the potential of the proposed framework for automotive applications.**

## I. Introduction

Over the last few years, automotive safety systems have become an intensive domain of research for Radio Frequency (RF) engineers. Vehicles are equipped with mobile communication systems in order to share information about the traffic conditions, current events concerning the traffic flow and possibly less critical data such as news and entertainment services. Development of these vehicle to vehicle (V2V) communication systems has made vast progress recently.

In current technological developments, RF front-end architectures in radar and wireless communications technologies are becoming more and more similar. In particular, the carrier frequencies used for communication systems, have shifted to the microwave regime and have become of the same order of magnitude as those traditionally used for radar applications [1]. Using one system to do both radar and communication can therefore be a more straightforward and beneficial concept, and has in fact been proposed repeatedly in the past [1].

In [2], [3], the authors presented a new joint radar-communication system based on the FrFT. The system is designed by taking into account the radar requirements, such as range and Doppler resolution, desired Side Lobe Levels, and the ability to reach data rates as high as 3.660 Mb/s while maintaining similar radar performance compared to a Linear Frequency Modulation (LFM) pulses that occupies the same bandwidth. The system proposed in [2], [3] has also been experimentally validated, however, it does not fit the standards of automotive radar and communication operation as it employs pulsed waveforms. The advantage of Continuous Waveform (CW) is that it can operate in lower peak power as the transmission is continuous. Additionally, CW radar are not restricted by minimum detectable range as the receiver is always operating. With respect to the communications aspect, CW is preferable as it provides 100% of duty cycle for the transmission meaning that the channel is fully occupied in time. Frequency Modulation Continuous Waveform (FMCW) transmission, is the most popular solution in automotive, exploiting both the advantages of CW and ranging capabilities of LFM signals.

Orthogonal Frequency-Division Multiplexing (OFDM) signals have become a popular choice in recent wireless communications standards, due to their robustness against fading and multipath propagation effects [1]. In [4], [5] the authors proposed an approach based on OFDM for joint radar-communication operation in automotive environment. While being a straight forward approach, the performance of the system is highly dependent on the good time and frequency synchronisation, the measurements are not accurate if the channel changes during the transmission of one OFDM symbol and inclusion of an equaliser increases the complexity in terms of the receiver processing.

In [6] a novel multi-carrier order division multi-access communication system is proposed based on Transform Domain Communication Systems (TDCS) with FrFT scheme, in which each user is uniquely identified by an FrFT order. This system is proposed to solve the multiple chirp carriers inter-shielding, which influences FrFT-OFDM demodulation performance.

In [16] the authors presented a Frequency modulation with rapid chirps on automotive radar systems. The rapid chirp waveform described in [16] meets the performance requirements on automotive radar systems almost perfectly. The simultaneously measurement of target range and radial velocity is very accurate since only frequency measurements are involved. Furthermore, the determination of target parameters is unambiguous even in multitarget situations, however this modulation does not support the communication functions.

In this paper the FrFT will be used to generate a chirp-like waveform, embedding information in the time-frequency domain and thus enabling communication functions in a manner similar to the one proposed in [3]. The contribution of the presented work can be summarised as: rather than exploiting the fractional order diversity to improve data transition rates [2], in the proposed scheme multiuser operations are allowed by assigning a specific order of the FrFT to each user. In this way it is possible to allocate more users in the same bandwidth with the advantage that the range resolution is not depended from the number of user that share the same bandwidth but only from order of the FrFT. Additionally, to allow CW operations a sample deletion and a Coherent

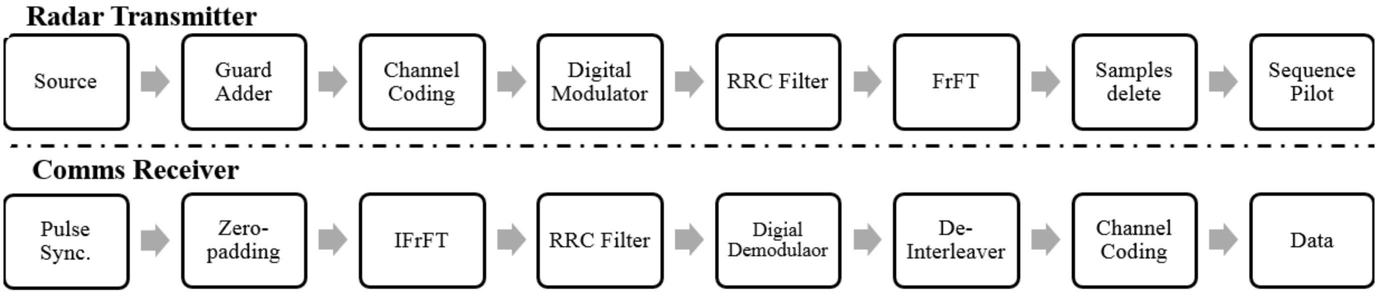


Figure 1: Block diagram of (top) the Radar Transmitter, in charge of the waveform generation, and (bottom) the Communication Receiver, whose task is demodulation of the received waveform

Processing Interval (CPI) operation are proposed. Finally, to resolve the problem of the synchronization a sequence pilot is mapped at the beginning of each transition instead of each pulsed as proposed in [2].

Other approaches based on joint Radar and Communication systems are presented in literature, however, these requires phased array and more advanced hardware solutions making them more suitable for larger radar systems (e.g. multi-function surveillance systems). In [13] a dual-function system based on time-modulated array is proposed, which implements the radar function in the main lobe while the communication is performed in the side lobe by exploiting the variation of the beam pattern. While, in [14] information embedding is achieved using sidelobe Amplitude-Shift Keying (ASK). Similar idea is presented in [15] wherein each orthogonal waveform embeds one information bit, whose value depends on the radiation pattern employed.

The remaining of the paper has the following structure. Section II introduces the FrFT, Section III describes the new system while in Section IV a comparison between the proposed and a LFM waveform is held in terms of ambiguity function (AF) and of Side Lobe Levels (SLL). In Section V the communication performance and a link budget for the proposed system are presented. Finally, Section VI concludes the paper.

## II. Fractional Fourier Transform

The FrFT belongs to the class of linear time-frequency representation (TFRs), and it was firstly introduced in [7]. The FrFT transforms a function into any intermediate domain between time and frequency. The $\alpha$-order FrFT is a linear operation defined as [8]:

$$\mathbf{X}_\alpha[u] = \sum_{u=-U/2}^{U/2} K_\alpha[u,u'] x[u'] \tag{1}$$

where $x[u]$ is an arbitrary signal of the length $U$ and $\alpha$ is the fractional Fourier transform order:

$$\alpha = \frac{2\phi}{\pi} \tag{2}$$

$\phi$ is the angle of rotation between time and frequency and $K_\alpha[u,u']$ is the FrFT kernel defined as [8]:

$$K_\alpha[u,u'] = \begin{cases} A_0 e^{j\pi\left(u^2+u'^2\right)\cot\phi} \\ \quad \times e^{-j\pi 2uu' \csc\phi} & \text{if } \phi \neq m\pi \\ \delta[u-u'] & \text{if } \phi = 2m\pi \\ \delta[u+u'] & \text{if } \phi = 2m\pi+\pi \end{cases}$$

where $A_0 = \frac{e^{j\frac{\phi}{2}}}{\sqrt{j\sin\phi}}$, $\delta[\cdot]$ is the Dirac delta function, $j=\sqrt{-1}$ and $m \in Z$ is an integer. The FrFT is an invertible linear transform, continuous in the angle $\phi$. In this paper, the FrFT is used as a tool to generate waveforms for joint radar and communication in automotive radar.

## III. Waveform Design

The waveform design process is illustrated in Fig. 1. A source generates $N$ bits of information and for $N$ bits, $G$ guard bits are added at the end of the sequence in order to compensate for the group of delay introduction by the Root Raised Cosine (RRC) filter. Then the sequence is spread by using a $L$-long Barker code, leading to a coded sequence of $(N+G)\times L$ bits. The interleaver[1] is used for burst error-correction. It is applied only to the $N \times L$ bits of information and aims to spread a burst of errors across the entire spread sequence. The digital modulator is the Frequency-Shift Keying (FSK) in which digital information is transmitted through discrete frequency changes of a carrier signal. This scheme assigns $N_s$ number of samples per symbol and for each symbol assigns a bandwidth $f_{sep}$, leading to $(N+G)\times L \times N_s$ long symbol sequence. In this system the FSK is used because it exhibits lower Side Lobe Levers compared to other approaches such as phase shift keying (PSK), [9]. The RRC filter is used to minimise the Inter-Symbol Interference (ISI) that may be caused by the channel. For efficiency, it is implemented as a multirate filter that up-samples the output by a factor $R_s$, leading to a final sequence of $U = (N+G)\times L \times N_s \times R_s$ samples. The time duration of the waveform after FrFT is:

$$T_{wave} = U/F_s \tag{3}$$

[1]The interleaver is applied to mitigate the impact of burst of errors in scenarios with strong fading.

where $F_s$ is sampling frequency.

The sequence obtained after applying the RRC filter is then mapped into a chirp in the time-frequency domain, with a specific order $\alpha$ of the FrFT. In automotive application, there will be interference issues due to the multiple signals transmitted from the radars on the adjacent driving vehicles operating in the same area at the same time. The use of the FrFT for this scenario has the advantage that every user is identified by a unique FrFT order and in the same area will be possible to allocate more users with different order $\alpha$ of the FrFT [6], [10], [11].

The module of the FrFT output transformed waveform is highly depended on the applied fractional order $\alpha$. In particular, as the order moves from 0 to 1 the energy of the waveform tends to concentrate at the center of the pulse. In Fig. 2 the absolute value of a constant modulus waveform is illustrated after applying FrFT of two different orders. Observing Fig. 2a and Fig. 2b it can be seen that as the energy concentrates in the middle of the waveform ($T_{wave}/2$), very low intensity samples appear at the beginning and end of the pulse. For this reason,

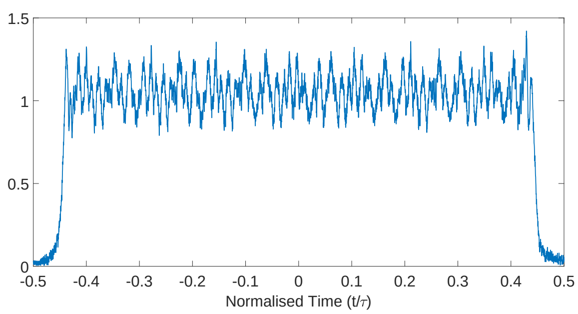


(a) with order of FrFT $\alpha = 0.3$.

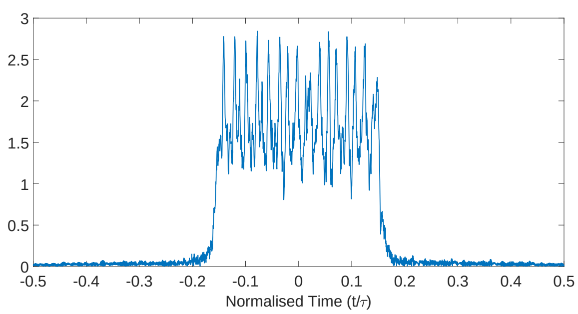


(b) with order of FrFT $\alpha = 0.8$.

Figure 2: Envelope of two signals with two different orders of the FrFT in particular as 2a) the $\alpha = 0.3$ and 2b) the $\alpha = 0.8$.

after applying FrFT, the waveform goes through a sample remove process where a fixed threshold is used to determine if a sample has a low enough intensity to be removed.

The spectrogram of a Coherent Processing Interval (CPI) after the samples delete stage is shown in Fig.3. For a single CPI, the same bits of information are mapped in every waveform and the same fractional order $\alpha$ is used. In this way it is possible to increase the Signal to Noise ratio (SNR) and therefore improve the radar performance. The bits of information change respectively from CPI to CPI. Finally, a pilot sequence is appended, employing code division multiplexing. The pilot waveform is embedded in the 0-th fractional order and it is transmitted at the begging of the communication for synchronisation with the receiver and for user/transmitter identification. Specifically, the pilot sequence is a bi-phase coded signal modulated by a Coarse/Acquisition (C/A) code [12] given by:

$$p[n] = e^{j\pi\left(a[n]-\frac{1}{4}\right)} \tag{4}$$

where $a[n]$ is up-sampled.

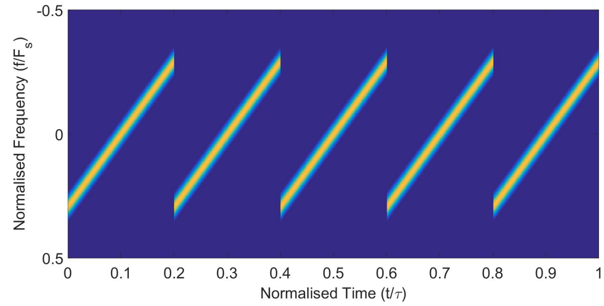


Figure 3: Spectrogram of a Coherent Processing Interval (CPI).

### A. Receiver

The communication receiver processing steps are shown in Fig. 1. The synchronisation is necessary to perform the inverse FrFT [2]. Once the synchronisation is performed, the waveform can be demodulated. The length of the input of the Inverse FrFT (IFrFT) must be the same length of the signal after the FrFT in transmission. For this reason a zero-padding is applied at the beginning and at the end of the received signal. The zero-padding leads to a sequence of $(N+G)\times L\times R_s\times N_s$ samples, that enters in IFrFT block to perform the inverse FrFT. The sequence is then passed to the RRC filter, which also down-samples the waveform by a factor $R_s$. The digital demodulator translates the $(N+G)\times L\times N_s$ long sequence of symbols in a sequence of $(N+G)\times L$ bits, according to the employed modulation. At this point, the de-interleaver performs the inverse of the interleaver. The chip correlator block correlates the input spread sequence with the $L$-long Barker code used in transmission to extract $N$ bits, exploiting both the low correlation side lobes and the knowledge that the peaks of the correlation occur every $L$ samples. In this way the $N$ bits of information can be recovered.

## IV. Performance Evaluation

In this section the radar performance of the proposed system is evaluated and compared with LFM waveforms. Two principal cuts of the ambiguity function (AF) have been considered to assess the radar performance. Namely, the zero-Doppler and zero-delay cuts of the AF will be used. The zero-Doppler cut is the autocorrelation function of signal transmitted, while the zero-delay cut is the Fourier transform of the magnitude

Table I: Simulated System Parameter

| Parameters | Description | Values |
|---|---|---|
| $f_c$ | Operating frequency. | 77 GHz |
| $M$ | Modulation order. | 2 |
| $f_{sep}$ | Frequency separation. | 9 MHz |
| $N_s$ | Number of sampler per symbol. | 2 |
| $F_s$ | Sampling Frequency. | 150 MHz |
| $\beta$ | Rolloff factor. | 0.8 |
| $S$ | Filter Span in Symbol. | 2 |
| $R_s$ | Output Samples per Symbol. | 13 |
| $L$ | Length of Barker code. | 7 |
| $R$ | Bit rate. | 0.7 Mbps |

squared of the complex envelope of the signal transmitted. The Side Lobe Levels (SLL) of the FrFT's and LFM are computed over 100 Monte Carlo runs for values of between 0 and 1 since the waveform characteristics are data dependent. For each order $\alpha$ the maximum, mean and minimum SLLs for the two AF cuts are calculated. The parameters of the simulated system are reported in Table I. The LFM is designed such that it has the same bandwidth and duration of the FrFT based waveform. Generally, when the order $\alpha$ moves from 0 to 1 the occupied bandwidth increase while the duration decreases [8]. Fig. $4a$ and Fig. $4b$ show the average AF, on

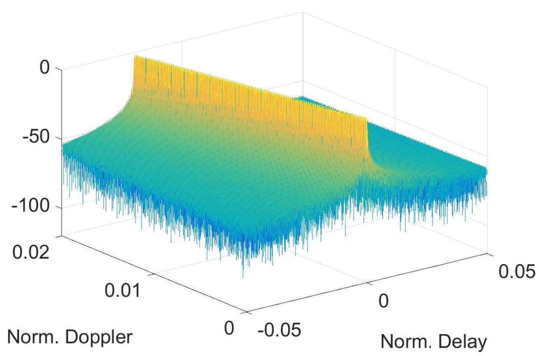


(a) FrFT ambiguity function.

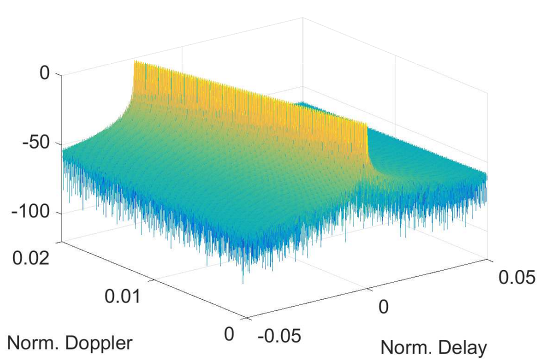


(b) LFM ambiguity function.

Figure 4: Average Ambiguity Functions (AFs) of the 4a) FrFT and 4b) LFM with same bandwidth and time duration.

100 iterations, of the FrFT and LFM respectively. The AF are computed with $\alpha = 0.5$. The FrFT AF has a similar shape

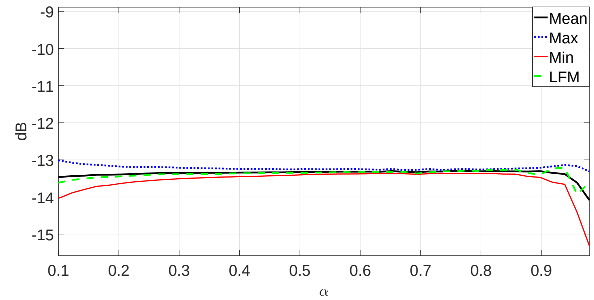


(a) SLL of the zero Doppler cut for the FrFT and LFM waveform.

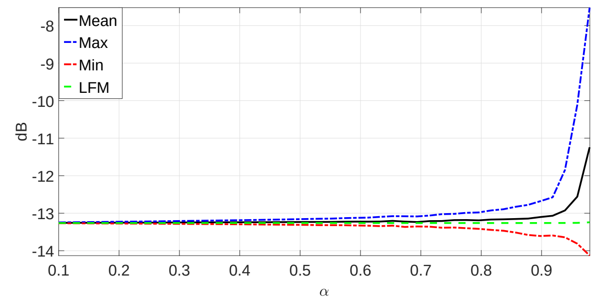


(b) SLL of the zero delay cut for the FrFT and LFM waveform.

Figure 5: Side Lobe Levels for different orders of the FrFT.

like the LFM AF. The SLL for zero-Doppler cut are shown in Fig. 5a, specifically for intervals $\alpha \in [0, 0.3]$ and $\alpha \in [0.9, 1]$ there is a large difference between the maximum and minimum values, because for this values of $\alpha$ the autocorrelation depends more on the Digital Modulator and less on the FrFT, while for $\alpha \in (0.3, 0.9)$ the values of maximum and minimum are very close because in this interval the autocorrelation depends more on the FrFT and less on the Digital Modulator. The SLL for the zero-delay cut are shown in Fig. 5b, where for $\alpha \in [0, 0.6)$ the values of the maximum and minimum are very close while for $\alpha \in [0.6, 1]$ there is a large difference between the maximum and minimum values, in particular when $\alpha < 0.6$ the magnitude squared of the complex envelope depends more from the Digital Modulator and less from the FrFT.

## V. Communication Performance

In this section, the communication performance is examined for different values of $SNR$ in terms of Bit Error Rate (BER), defined as the ratio between the number of bits wrongly decoded and the total number of bits sent. Moreover, a link budget analysis is performed in order to demonstrate the applicability of the proposed FrFT based waveform design method in automotive environment.

The performance of the communication systems in terms of BER are evaluated considering Additive White Gaussian Noise (AWGN). The probability of bit error for coherently detected orthogonal Binary FSK (BFSK) in an just AWGN channel in [1] is:

$$P_{be,BFSK} = Q\left(\sqrt{\frac{E_b}{N_o}}\right) = \frac{1}{2} erfc\left(\sqrt{\frac{E_b}{2N_o}}\right) \tag{5}$$

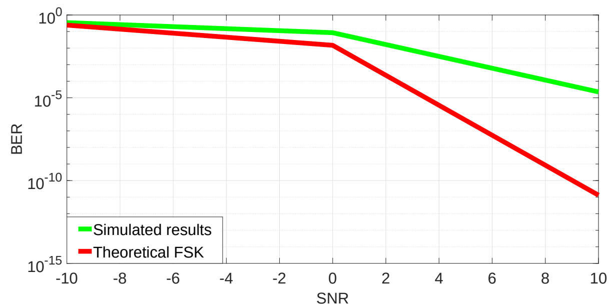


Figure 6: Performance in terms of BER of the FrFT waveform in presence of AWGN.

where $Q$ is the Q-function, $erfc$ is the complementary error function while $E_b$ and $N_o$ are energy per bit and energy of the noise respectively.
In the Fig. 6 the theoretical FSK and simulated results are compared. The curve is obtained of a Monte Carlo simulation during which $10^8$ bits are sent whit order $\alpha = 0.5$ and for $SNR = [-10, 0, 10]$. With a $SNR$ equal to 10 dB the theoretical BER is $1.3 \cdot 10^{-11}$ while the simulated one is $2.259 \cdot 10^{-5}$. The Fig. 6 show that the BER simulated is a good approximation of the theoretical FSK.

### A. Link Budget

In the following, the link budget and radar equation for the communication and radar applications are calculated. The $SNR$, is chosen depending on the desired radar and communication performance. Typical system parameters and requirements are summarized in Table II. The maximum radar range, $r_{max}$, and the maximum radar-communication receiver distance, $d_{max}$ are obtained. For this specific analysis, the radar link budget is obtained by rearranging the radar range equation as follows:

$$r_{max} = \sqrt[4]{\frac{P_t}{\tau} \frac{G_t G_{r,radar} \lambda^2 \sigma}{(4\pi)^3 F k T_0 B_w SNR_{radar}}} \tag{6}$$

$$d_{max} = \sqrt{\frac{P_t}{\tau} \frac{G_t G_{r,comms} \lambda^2}{(4\pi)^2 F k T_0 B_w SNR_{comms}}} \tag{7}$$

For the communication a $SNR_{comms} = 10$ dB secure a $BER = 10^{-5}$. In the same time, a data stream of 0.7 Mb/s can be directed to a communication receiver placed at a distance of 1.26 km. For the radar when $SNR_{radar} = 8$ dB, and a target with radar cross section of 1 $m^2$ can be detected at a maximum range of 79.72 m. Typically, in an automotive environment multiple users shall be able to communicate with each other. In cases where the users are in close proximity, different fractional orders can be allocated in each user. Additionally, those fractional orders can be reused in cases where the users are at higher distance than $d_{max}$.

Table II: Link Budget Parameters

| Parameters | Description | Values |
|---|---|---|
| $P_t$ | Transmitted power. | 20 dBm |
| $G_t$ | Radar Transmitting Antenna Gain. | 30 dB |
| $\lambda$ | Wavelength. | 0.389 cm |
| $k$ | Boltzmann's constant. | 1.38 $\times 10^{-23} J/K$ |
| $T_0$ | Noise reference temperature. | 290 K |
| $\sigma$ | Radar cross section. | $1 m^2$ |
| $F$ | Radar and communication noise figure. | 5 dB |
| $\tau$ | Duty cycle. | 1 |
| $G_{r,comm}$ | Communication Receiver Antenna Gain. | 5 dB |

## VI. Conclusion

This paper presented a new system for joint radar and communication in automotive radar. The framework performance was evaluated in terms of AF and SLL. Simulation analysis showed that the proposed system can achieve similar performance to LFM while also enabling communication capabilities. Communication performance and link budgets have also been assessed and the results suggest that the proposed system can be employed for reliable communication. Future developments include, coexistence/interference analysis for this new waveform design and sensitivity to adjacent/co-channel interference from colored noise.


## Acknowledgements

This work is supported by NXP Laboratories UK Limited and by the Engineering and Physical Sciences Research Council (EPSRC) Grant number EP/K014307/1 and the MOD University Defence Research Collaboration in Signal Processing.


## References


[1] C. Sturm, W. Wiesbech, "Waveform Design and Signal Processing Aspects for Fusion of Wireless Communications and Radar Sensing", *IEEE journals & Magazines*, vol.99, pp.1236-1259,2011.

[2] D. Gaglione, C. Clemente, C. V. Ilioudis, A. R. Persico,I. K. Proudler, J.J.Soragan "Fractional Fourier Based Waveform for a Joint Radar-Communication System.", *IEEE Radar Conference*, 2016.

[3] D. Gaglione, C. Clemente, C. V. Ilioudis, A. R. Persico,I. K. Proudler, J.J.Soragan "Fractional Fourier Transform Based Co-Radar Waveform: Experimental Validation.", *Sensor Signal Processing for Defence (SSPD)*, pp. 1-5, 2016.

[4] S. Patole, M. Torlak, D. Wang, and M. Ali, "Automotive Radars A review of signal processing techniques.", "Signal processing for smart vehicle technologies: part 2", *IEEE Signal Processing Magazine*", 2017.

[5] C. Sturm, E. Pancera, T. Zwick, and W. Wiesbeck,"A Novel Approach to OFDM Radar Processing.", *IEEE Radar Conference, 2009*, 2009.

[6] Z. Yang, R. Tao, Y. Wang, T. Wang, "A Novel Multi-carrier Order Division Multi-access Communication System Based on TDCS with Fractional Fourier Transform Scheme.", *Springer Science+Business Media New York 2014, Wireless Pers Commun (2014) 79:130.1-1320*, 2014.

[7] V. Namias, "The Fractional Order Fourier Transform and its Application to Quantum Mechanics.", *IMA Journal of Applied Mathematics*, vol.25, no.3, pp.241-265, 1980.

[8] H. M. Ozaktas, Z. Zalevsky, and M. A. Kutay,"The Fractional Fourier Transform with Applications in Optics and Signal Processing." Wiley, Chichester, 2001.

[9] S. Mi, X. Liu, and Z. Qu, "Recognition of Radar Signal Modulation Based on Fractional Fourier Transform.", *International Journal of Signal Processing System*, Vol. 25, No.2, 2017.

[10] C. Clemente, C. Ilioudis, D. Gaglione, K. Thompson, S. Weiss, I. Proudler, J.J. Soraghan, "Reuse of fractional waveform libraries for MIMO radar and electronic countermeasures.", *2014 6th International Symposium on Communications, Control and Signal Processing (ISCCSP)*, 2014.

[11] C. Ilioudis, C. Clemente, I. Proudler, J.J. Soraghan, "Performance analysis of fractional waveform libraries in MIMO radar scenario.", *Radar Conference (RadarCon), 2015 IEEE*, 2015.

[12] GPS ICD,"Global Positioning Systems Directorate System Engineering & Integration Interface Specification IS-GPS-200H.", *Navstar GPS Space Segment/Navigation User Interfaces*, 2013.

[13] J. Euzire, R. Guinvarch, M. Lesturgie, B. Uguen, R. Gillard, "Dual Function Radar Communication Time-Modulated Array.",*2014 International Radar Conference (Radar)*, Lille, France, 2014, pp. 1-4

[14] Muharrem Arik, Ozgur B. Akan, "Utilizing sidelobe ASK based joint radar-communication system under fading.", *MILCOM 2017 - 2017 IEEE Military Communications Conference (MILCOM)*, 2017, pp. 623-628.

[15] A. Hassanien, M. G. Amin, Y. D. Zhang, F. Ahmad, "Dual-Function Radar-Communications: Information Embedding Using Sidelobe Control and Waveform", *IEEE Transactions on Signal Processing 64 (8).*, 2016, pp. 2168,2181. Diversity

[16] F. Gini, A. De Maio and L. Patton, "Waveform Design and Diversity for Advanced Radar Systems.", *IET Radar, Sonar and Navigation Series 22*, 2012.

[17] "Link Budget Analysis: Digital Modulation.", *www.AtlantaRF.com*, 2012.